DOI: 10.1002/ejic.200701284

Base-Induced Formation of Two Magnesium Metal-Organic Framework Compounds with a Bifunctional Tetratopic Ligand

Pascal D. C. Dietzel,*[a,b] Richard Blom,[a] and Helmer Fjellvåg[b]

Keywords: Microporous materials / Coordination polymers / Metal-organic frameworks / Organic-inorganic hybrid composites / Adsorption / Magnesium / X-ray diffraction / Hydrothermal synthesis / 2,5-Dihydroxyterephthalic acid

Two coordination polymers constructed from magnesium and the tetratopic organic linker 2,5-dihydroxyterephthalic acid are reported, denominated CPO-26-Mg and CPO-27-Mg. The organic component carries two different types of protic functional groups. The degree of deprotonation of the organic component can be regulated by the amount of sodium hydroxide employed in the synthesis, thus determining which of the compounds forms. In CPO-26-Mg, only the carboxylic acid groups of the linker are deprotonated and take part in the construction of the three-dimensional framework. The structure is non-porous, and its topology is based on the PtS net. In CPO-27-Mg, both the carboxylic acid and the hydroxy groups are deprotonated and involved in the construction of a microporous three-dimensional framework which is based on a honeycomb motif containing large solvent-filled channels. The metal atoms are arranged in chiral chains along the intersection of the honeycomb and contain one water molecule in their coordination sphere, which allows for the creation of coordinatively unsaturated metal sites upon dehydration. CPO-27-Mg is a potentially useful lightweight adsorbent with a pore volume of 60 % of the total volume of the structure and an apparent Langmuir surface area of up to 1030 $m^2 g^{-1}$. Its thermal stability was investigated by thermogravimetry and variable-temperature powder X-ray diffraction, which shows framework degradation to commence at 160 °C in air, at 235 °C under nitrogen, and at 430 °C in a dynamic vacuum. Thermogravimetric dehydration and rehydration experiments at miscellaneous temperatures indicate that it is possible to obtain open metal sites in CPO-27-Mg, but the water is more tightly bound in this material than in the previously reported isostructural nickel compound.

Introduction

Porous coordination polymers, or metal-organic frameworks, are extremely interesting substances for the storage of gases or other adsorbates because of their high specific surface area and pore volume.[1–5] For the storage of light gases, like hydrogen, to be economical, the mass of the empty framework should be as minimal as possible. One way to achieve this is with frameworks with an extremely high pore volume.[6–13] However, it has been postulated that hydrogen is optimally stored in porous materials with pore diameters of ca. 6 Å.[14] Frameworks with extremely high pore volumes usually also have very large pore diameters, which then might adversively affect the adsorption properties, e.g. by reducing the selectivity or even inhibiting large adsorption values. An alternative possibility of decreasing the specific weight of the framework is by using building blocks which are as lightweight as possible. Since the organic component already consists of light elements, this leaves the metal component as the sole parameter that can be optimized. Many coordination polymers contain divalent transition metals as metal component. Magnesium is one of the lightest metals, and it is therefore theoretically an ideal choice for the construction of possibly non-toxic and lightweight frameworks. However, relatively few magnesium coordination polymers are reported among the wealth of literature describing novel MOFs.[15–37]

In this paper, we present the synthesis and characterization of two coordination polymers formed by reaction of magnesium nitrate and 2,5-dihydroxyterephthalic acid (H_4dhtp), a tetratopic ligand that carries two different types of functional groups. It has been used previously to prepare microporous frameworks containing the metals zinc, cobalt, nickel, and scandium.[38–42] Which of the two framework compounds is formed depends on the extent to which the ligand is deprotonated, and it may be adjusted by the amount of base employed in the synthesis. One of the metal-organic frameworks is non-porous, while the other exhibits microporosity. We report the thermal stability of the latter framework, its congruent ability to reversibly release and adsorb again the water contained in its pores, and its behavior towards nitrogen gas adsorption.

[a] SINTEF Materials and Chemistry,
P. O. Box 124 Blindern, 0314 Oslo, Norway,
E-mail: pascal.dietzel@sintef.no
[b] Centre of Materials Science and Nanotechnology, Department of Chemistry, University of Oslo,
P. O. Box 1033 Blindern, 0315 Oslo, Norway

Supporting information for this article is available on the WWW under http://www.eurjic.org or from the author.

Results and Discussion

Syntheses

2,5-Dihydroxyterephthalic acid contains two types of protic functionalities: (i) two carboxylic acid groups, (ii) two hydroxy groups. Phenolic protons are significantly more acidic than aliphatic alcohols. Thus, they can be easily deprotonated by a sufficiently strong base. Alternatively, the resulting framework compound itself may be sufficiently stable to promote the formation of the framework containing the deprotonated hydroxy group, as we have observed during the syntheses of the cobalt and nickel compounds $[M_2(dhtp)(H_2O)]\cdot 8H_2O$, CPO-27-M (M = Co, Ni),[39,41] where the final pH value is weakly acidic (ca. 5–6).

In the present case, the ratio of base/organic ligand determines whether only the carboxylic acid groups are deprotonated or all the protic groups of the ligand are in their deprotonated form. For reasons of charge neutrality, the ratio of magnesium/ligand is 1:1 in CPO-26-Mg, whereas it is 2:1 in CPO-27-Mg. The organic solvent, ethanol and THF for CPO-26-Mg and CPO-27-Mg, respectively, used in the experimental procedure given below was chosen to increase the yield of the reaction. The respective product is also obtained when the organic solvents are interchanged. (However, in the case of CPO-26-Mg, only very few yellow crystals are obtained with THF instead of ethanol in the solvent mixture.)

It is noteworthy to mention that in the case of cobalt and nickel, we only obtained the 2:1 compounds even under conditions which are supposed to favor the formation of the 1:1 compounds, whereas it is also possible to induce the formation of a 1:1 and a 2:1 compound by selective deprotonation of the organic acid with zinc as cation.[40,43]

Crystal Structures

Of the protic functional groups of 2,5-dihydroxyterephthalic acid only the carboxylic acid groups are deprotonated in CPO-26-Mg. Hence, only the carboxylate groups of the ligand are involved in the coordination of the magnesium atom, while the hydroxy groups form intramolecular hydrogen bonds with the oxygen atoms of the adjacent carboxylate groups. Each of the oxygen atoms of the carboxylate group coordinates a magnesium atom; the carboxylate groups thus function as bridging connector between isolated octahedra of magnesium atoms surrounded by oxygen atoms, four of which belong to carboxylate groups and the remaining two belong to two water molecules in *cis* orientation to each other. The magnesium coordination octahedra linked in this way form zigzag chains (Figure 1a). The chains are linked by the organic ligand such that a three-dimensional framework results in which the chains are oriented in parallel (Figure 1b). The planes of the phenyl rings are arranged in a staggered conformation on top of each other and in parallel with a distance of 3.499(2) Å between their centers of gravity. Selected bond lengths and angles are listed in Table 1. The hydrogen atoms of the water molecules are involved in hydrogen bonding to oxygen atoms of the hydroxy groups of the organic ligand (Table 2).

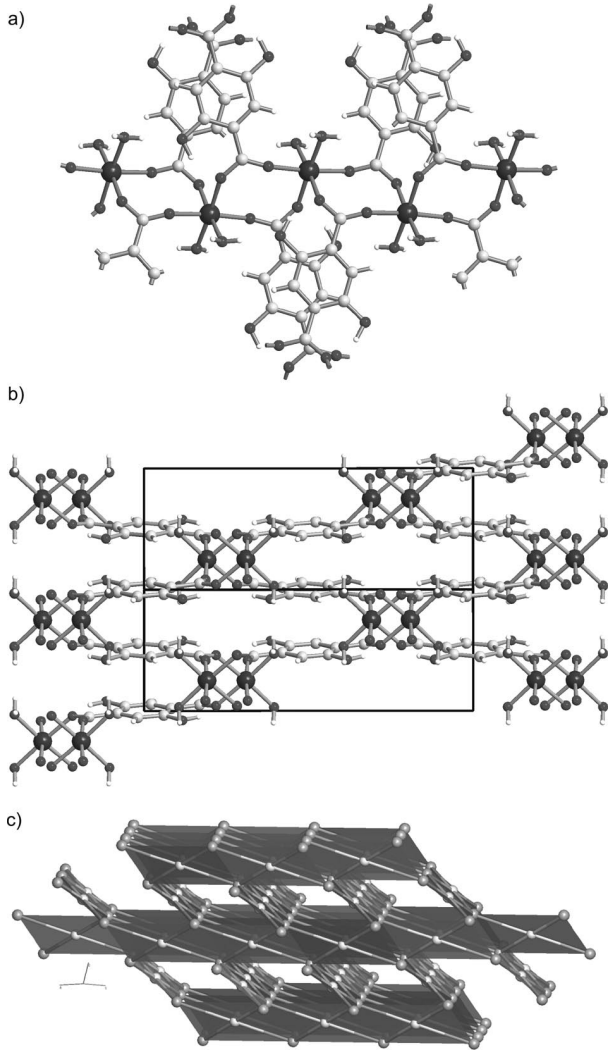

Figure 1. Crystal structure of CPO-26-Mg: (a) coordination geometry around the magnesium atom and chains formed by the bridging carboxylate groups; (b) three-dimensional framework viewed along the chains of magnesium–oxygen octahedra linked in this way; (c) topological representation.

Topologically, each metal building block is connected to four of the organic linker building blocks and vice versa; thus, they form a [4,4] net. Whereas the connections of the organic ligand are planar, the environment of the magnesium resembles a compressed tetrahedron. The tetrahedron-like polyhedra form chains by sharing two edges each with adjacent polyhedra which are then linked three-dimensionally through common vertices. However, the topology is better described by using the planar tiles formed by the metal atoms surrounding the organic ligand. The tiles form edge-sharing chains along the two diagonals of the *ab* plane. The normal vector of these planar chains is tilted in respect to the *ab* plane. The chains in the two diagonal

Table 1. Selected geometric parameters for CPO-26-Mg and CPO-27-Mg (distances in Å, angles in °).

CPO-26-Mg			
Mg1–O1	2.0810(15)	C1–O2	1.246(2)
Mg1–O2	2.0254(14)	C1–O1	1.272(2)
Mg1–O4	2.0892(15)		
O2–Mg1–O1	94.31(6)	O2–Mg1–O4	89.74(6)
O2–Mg1–O1	89.23(5)	O2–Mg1–O4	86.96(6)
O2–Mg1–O1	89.23(5)	O1–Mg1–O4	89.32(6)
O2–Mg1–O1	94.31(5)	O4–Mg1–O4	94.49(9)
O1–Mg1–O1	86.90(9)	O2–C1–O1	124.07(16)
O2–Mg1–O4	86.96(6)	C1–O1–Mg1	133.53(11)
O2–Mg1–O4	89.74(6)	C1–O2–Mg1	156.30(12)
O1–Mg1–O4	89.32(6)		
CPO-27-Mg			
Mg1–O1	2.023(4)	Mg1–O3	1.974(4)
Mg1–O2	2.070(4)	Mg1–O4	2.148(4)
Mg1–O2	2.166(4)	O1–C1	1.307(5)
Mg1–O3	2.108(4)	O2–C1	1.238(6)
O1–Mg1–O2	95.43(16)	O1–Mg1–O3	96.96(18)
O1–Mg1–O3	99.16(17)	O1–Mg1–O4	92.76(17)
O2–Mg1–O2	80.18(9)	O2–Mg1–O3	81.80(15)
O2–Mg1–O3	81.73(17)	O2–Mg1–O4	91.69(16)
O2–Mg1–O3	90.92(19)	O2–Mg1–O3	82.59(15)
O3–Mg1–O4	90.53(18)	O3–Mg1–O4	93.69(19)
Mg1–O2–Mg1	95.15(13)	Mg1–O3–Mg1	96.72(13)
O1–C1–O2	125.8(5)		

Table 2. Short intermolecular distances pertaining to hydrogen bonds in CPO-26-Mg.

D–H···A	D–H	H···A	D···A	<(D–H···A)
O3–H3···O1 (intra)	0.91(3)	1.69(3)	2.520(2)	151(3)
O4–H4···O3	0.80(3)	2.03(3)	2.818(2)	170(3)
O4–H5···O3	0.87(3)	2.03(3)	2.885(2)	170(3)

directions are connected by common corners, thus forming the three-dimensional framework. The resultant topology is of the PtS type (Figure 1c).

CPO-27-Mg is isostructural with the corresponding compounds of zinc, cobalt, and nickel,[38–41] as was already suggested by the similarity of the powder X-ray diffraction patterns. All functional groups of the ligand are deprotonated, and all of them are involved in coordination towards the magnesium atoms in the crystal structure (Figure 2a, see Table 1 for selected bond lengths and angles). The carboxylate group coordinates two metal atoms in pincing mode. One of its oxygen atoms coordinates an additional magnesium atom together with the oxygen atom of the deprotonated hydroxy group in α-position to the carboxylate group, hence forming a six-ring chelate complex. The oxido group also coordinates one more magnesium atom. Thus, each α-oxido carboxylate functionality of the ligand coordinates a total of four metal atoms. The magnesium atom is again surrounded in an octahedral fashion by oxygen atoms, with five of them belonging to a ligand. The sixth oxygen atom is part of a water molecule. The closely spaced arrangement of multiple metal atoms by the ligands results in condensed coordination polyhedra, specifically one-dimensional threefold helical chains of magnesium–oxygen octahedra which share common edges in *cis* position to each other (Figure 2a). Naturally, these chains are chiral, and one could envision stereoselective adsorption. However, the framework contains a racemic mixture of chains of both handednesses as a consequence of the presence of a center of inversion. The organic linker connects the helical chains in such a way that a honeycomb pattern results (Figure 2b), with the metal–oxygen chains at the intersections and leaving one-dimensional pores of close to 12 Å diameter which are filled with solvent water molecules (the diameter apparent to a probe molecule is naturally diminished by the probe molecule's own diameter, e.g. the diameter of the channels in CPO-27 "visible" to a nitrogen molecule with a kinetic diameter of 3.6 Å is in the range of 8–9 Å). The water molecule that is coordinatively bound to the magnesium atom points towards the cavity. The potentially removable water molecules occupy 60% of the total volume of the structure.

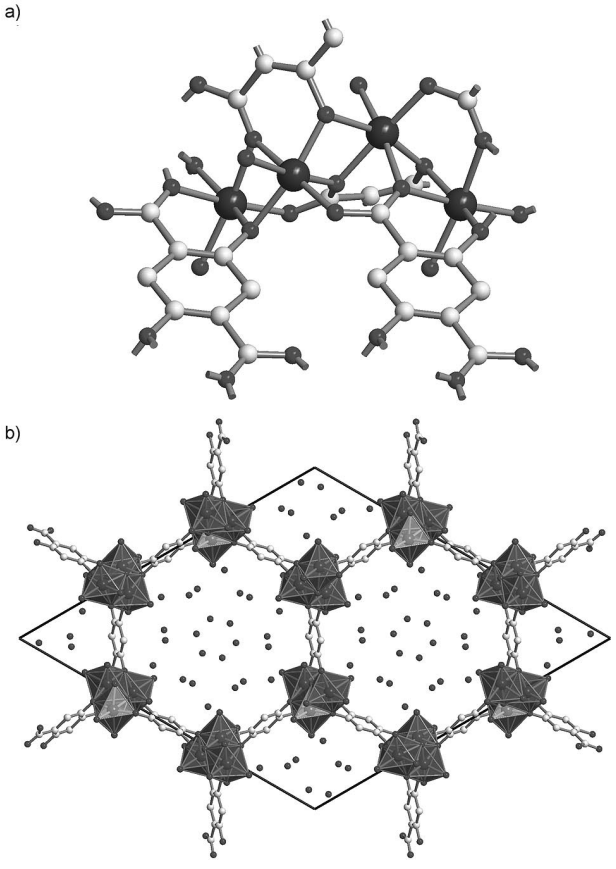

Figure 2. Crystal structure of CPO-27-Mg: (a) helical threefold chains of *cis*-edge-connected magnesium–oxygen coordination octahedra; (b) packing viewed along [001] showing the water-filled one-dimensional channels.

Naturally, the coordination number of the completely deprotonated dhtp ligand is twice as high as for the metal atoms in CPO-27-Mg. The networks are constructed of 4-gons around the metal atoms and 8-gons around the organic node. The 4-gons resemble strongly distorted tetrahe-

dra. They are linked by common faces to form trigonal pillars along the *c* axis. The pillars are then joined by common edges so that the hexagonal channels are left empty, and the topology is that of a 4,8-*c* net.

Thermal Stability

The TG curve of the porous CPO-27-Mg (Figure 3) shows an immediate reduction in weight as soon as the sample is exposed to the dry gas stream in the apparatus, which is coherent with the removal of the solvent water. The rate of decrease levels off above 100 °C. However, under nitrogen, the curve does not reach a plateau of constant weight, before decomposition to magnesium oxide occurs. In air, such a plateau is reached at 305 °C, just after a noticeable step. The relative mass of the plateau corresponds to the dehydrated compound Mg_2(dhtp). Starting shortly above 400 °C in both types of gases, a final step occurs, which corresponds to the decomposition of the framework and yields magnesium oxide as product as determined by powder X-ray diffraction and residual weight. Under nitrogen, it is especially apparent that decomposition proceeds before a level of constant mass equivalent to the fully dehydrated compound has been reached. This observation already points towards a potential difficulty in removing all of the water contained in the pores.

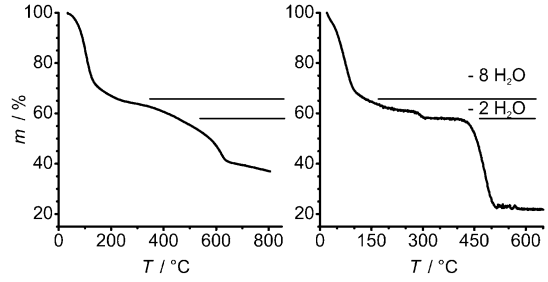

Figure 3. TG curve of CPO-27-Mg under nitrogen (left) and in air (right) with indication of the mass corresponding to the eight water molecules in the channels and the two water molecules which coordinate the magnesium atom.

While the decomposition of CPO-27-Mg to MgO under an inert gas and in air appears to occur at similar temperatures in the TG curves, pronounced differences become apparent in the variable-temperature powder X-ray diffraction which reveals the stability of the long-range order of the framework with increasing temperature (Figure 4). In both gases and in vacuo, the intensity of the first two (and strongest) reflections immediately increases noticeably during removal of the bulk of the water contained in the channels on initial heating. Afterwards, the maximum intensity of the first and strongest reflection remains constant within a temperature range dependent on the gas, indicating stability of the long-range order of the dehydrated framework. Finally, the maximum intensities of the reflections decrease and ultimately disappear, reflecting a loss of crystallinity of the framework. Under nitrogen, this occurs in the range of 235–324 °C, whereas it proceeds already in the range of 160–209 °C in air. These temperatures are significantly lower than the weight loss steps in the TG curves associated with decomposition of the dehydrated structure. The structural integrity is therefore lost earlier than the substance is actually burnt off. It should also be noted that it therefore would have been misleading to judge the thermal stability solely on the basis of the TG curves. However, crystalline CPO-27-Mg remains stable to a much higher temperature in a dynamic vacuum, in which the decrease of crystallinity is observed only above 430 °C.

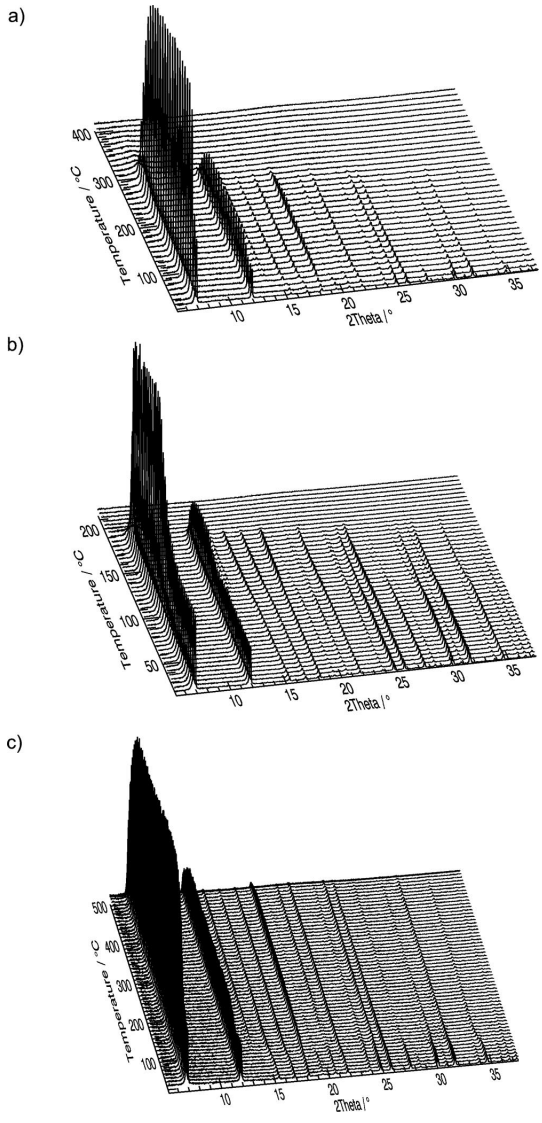

Figure 4. Variable-temperature powder X-ray diffraction of CPO-27-Mg under nitrogen (a), in air (b), and dynamic vacuum (c) showing the different temperature ranges in which the framework is stable (note the difference in scale of the temperature axes).

The variable-temperature powder X-ray diffraction clearly shows that the framework is stable at higher temperatures under an inert gas than it is in air, and at even higher temperatures in the absence of potential collision partners from the gas phase. The loss of crystallinity in

vacuo commences roughly at the same temperature at which decomposition is observed in the TG curves. However, in air and under nitrogen, the long-range order of the compound disappears at significantly lower temperatures. It is the amorphous product of the collapse of the framework which subsequently decomposes to MgO as metal-carrying species.

We have previously shown for the isostructural compounds CPO-27-Co, CPO-27-Ni, and CPO-27-Zn that the metal atom becomes coordinatively unsaturated in the dehydrated compounds and accessible from the evacuated pores.[39–41] In contrast, the water in CPO-27-Mg apparently has not been completely removed within the range of stability of the framework. In air, even though there is a plateau corresponding to the fully dehydrated material in the TG curve, it occurs above the temperatures for which the variable-temperature powder diffraction experiment indicates that the material is still crystalline. The comparison of TG and in-situ powder diffraction suggests that all of the non-coordinating water can be removed before the framework starts to collapse at 160 °C. Thus, it appears reasonable to assume that the collapse of the framework commences in step with the removal of the final water which is likely the magnesium-coordinating molecule. Its absence creates a reactive site at the metal atom, but because magnesium is not susceptible to redox reactions under the conditions present, we reason that the framework collapse must be related to the organic ligand, possibly involving reaction with oxygen from the air. The latter appears likely because the framework is stable to significantly higher temperatures under nitrogen, in which there is no oxygen present. Nonetheless, even under an inert gas, the coordinating water is not completely removed before framework degradation sets in. According to the experiments and the re-hydration experiment described below, more than 50% of the water molecules coordinating the magnesium atoms is removed, while the framework is still intact. Thus, a certain amount of open metal sites is expected to be present in CPO-27-Mg upon heating under these conditions.

Adsorption Properties

The thermogravimetric analysis indicates that the bulk of the water is easily removed from the pores, whereas the variable-temperature powder X-ray diffraction experiment reveals relatively little change in the reflection positions which suggests that the framework remains essentially unperturbed by dehydration. In combination, these findings indicate that the channels of the dehydrated structure are accessible for guest molecules. The initial and straightforward experiment to probe the accessibility is, of course, to attempt the re-hydration of previously dehydrated samples.

The experiment was performed under argon. First, the water was removed from the sample of CPO-27-Mg by heating to a specific temperature and keeping the sample at this temperature for some time in a TG apparatus. Afterwards, the heating was removed and the sample exposed to gas which was humidized by bubbling through a water-containing flask. For all temperatures investigated, 100, 150, and 200 °C, the sample took up the same amount of water it had released previously during heating (Figure 5), and it did so independently of the time spent tempering the sample. Consequently, the material is stable under these conditions for extended periods of time, and the desorption/adsorption process is fully reversible under the conditions employed. This ability correlates with the structural integrity of the framework, as shown for the analogous nickel compound previously.[41] There is a noteworthy difference to the analogous experiment for CPO-27-Ni, though. The amount of water removed by heating did not vary significantly in case of the nickel compound for the various tempering temperatures used, whereas it is approximately 4% less at 100 °C than at 200 °C for the magnesium compound, which corresponds roughly to one water molecule per formula unit. Even at 200 °C the final weight is slightly higher (60%) than expected for the completely dehydrated framework (57%). This clearly confirms the increased difficulty of removing the final metal-coordinating water molecules in case of the magnesium compound. The non-coordinating water molecules can be completely removed already at 100 °C, corresponding to 66% of the weight of the fully hydrated compound. Thus, in principle, access to the magnesium atom under mild conditions is possible for alternate guests that can substitute the coordinating water molecule, and, as mentioned above, there is a fair percentage of coordinatively unsaturated metal atoms present when the dehydration is performed under more rigid conditions under an inert gas.

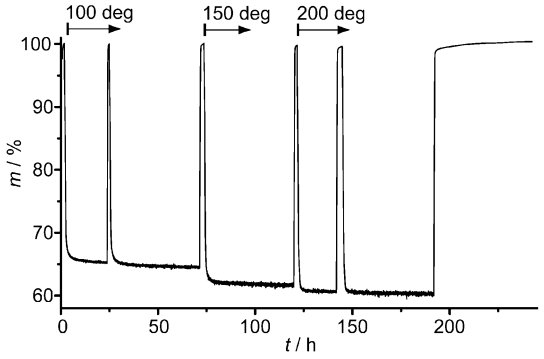

Figure 5. Reversibility of dehydration of CPO-27-Mg at various temperatures under nitrogen (re-hydration performed at room temperature in a humid stream of argon).

Aside from observing the ability to put solvent molecules back into the pores, porous materials are customarily probed by gas adsorption to assess the accessible surface area and pore volume. Because they are isostructural, the absolute surface area of CPO-27-Mg should be similar to that of its nickel analogue, CPO-27-Ni, for which an apparent Langmuir surface area of 1083 $m^2 g^{-1}$ and pore volume of 0.41 $cm^3 g^{-1}$ was measured by nitrogen gas adsorption.[41]

However, attempts to measure the apparent surface area of CPO-27-Mg by nitrogen gas adsorption delivered inconsistent results. Not only did the obtained values for the ap-

parent surface area of CPO-27-Mg vary widely, even with very similar pre-treatment conditions and identical sample batch, but in most cases the apparent surface areas were also significantly smaller than those of CPO-27-Ni. Still, some generalization can be made from these experiments. Significantly high surface areas cannot be obtained with a pre-treatment temperature of 110 °C, which is sufficient to completely remove the water from CPO-27-Ni and access its full surface area. Higher temperatures during activation are needed in the case of the magnesium compound to measure any significant amount of surface area. In addition, the correct activation of the sample in advance of pre-treatment appears to be crucial, e.g. by grinding or repeated washing with water or prior exchange with an alternate solvent like methanol (a Table with complete information of pre-treatment procedures is included in the Supporting Information). It is difficult to elucidate a clear-cut relationship between conditions and surface area. However, longer pre-treatment times and as high as possible activation temperatures generally seem to increase the apparent surface area, even though there are some outliers to this trend among the experimental data. We did observe porosity of comparable magnitude to CPO-27-Ni in a sample that had been subjected to several subsequent measurements and been stored in a dehydrated state under an inert gas for two weeks, before being re-hydrated just prior to the experiment. The experiment yielded an apparent Langmuir surface area of 1030 $m^2 g^{-1}$ (BET surface area: 877 $m^2 g^{-1}$) and a pore volume of 0.37 $cm^3 g^{-1}$ (Figure 6). (Note, however, that the surface area per mass should be larger by ~30% for the Mg compound in comparison to the Ni compound, if all of the internal surface area of the structure was accessible.) In this instance, CPO-27-Mg is the material with the highest apparent surface area among the porous magnesium-based metal-organic frameworks reported so far.[21,24,25] Unfortunately, we have been unable to reproduce this result to date. Usually, Langmuir surface areas in the range of 150–500 $m^2 g^{-1}$ are observed when the activation temperature was 200 °C or higher. It clearly seems to be very intricate to establish admission of the nitrogen probe molecule to the full micropore volume.

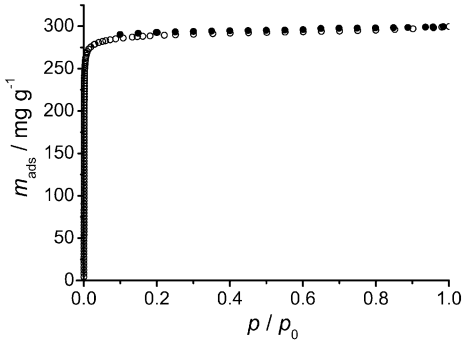

Figure 6. Best nitrogen adsorption isotherm of CPO-27-Mg (open circles: adsorption measurement; closed circles: desorption measurement).

The results of the re-hydration and gas adsorption experiment conflict to a certain degree with each other. The former shows facile accessibility of the pore structure, while difficulties are experienced in the latter. Still, the observation of high surface area and pore volume in a number of experiments supports the permanence of porosity. Rather, it appears likely that the cause for regularly encountered lower values in the adsorption experiment must lie elsewhere. One possibility could be in the nature of pore termination which might allow the polar water molecule to penetrate into the channels more easily than the non-polar nitrogen molecule. We think the most likely cause is the incomplete removal of water under the activation conditions. Even the application of high temperatures does not remove the water completely. Therefore, it might accumulate close to the pore openings under pre-treatment conditions and subsequently block the channels partly in the adsorption experiment at 77 K. When procedures are established to reliably access the full extent of the micropore volume, CPO-27-Mg can be used to store ca. 27 wt.-% more guest molecules than CPO-27-Ni by virtue of its lighter molecular mass. This is assuming the same amount of guest per volume, which may well increase for the magnesium compound because of stronger dispersion forces.

Like for the other CPO-27 compounds, re-hydration of CPO-27-Mg is an exothermic process to the extent that it is accompanied by a sizzling sound which resembles that of water evaporating when it drops on a hot stone. This effect is proportional to the accessible surface area observed in the preceding adsorption experiment.

Conclusion

A non-porous and a microporous metal-organic framework compound are formed from magnesium nitrate and 2,5-dihydroxyterephthalic acid depending on the degree of deprotonation of the organic linker, which is determined by the amount of base added in the synthesis. The microporous compound is isostructural with compounds containing zinc, cobalt, or nickel in place of magnesium. This family of materials can therefore be used to investigate how their properties are dependent on the respective metal component. The magnesium compound is potentially of special interest as adsorbent due to the combination of large pore volume and light weight. The bulk of the water consisting of the non-coordinating water molecules can be removed easily and reversibly as long as the framework structure is intact. However, the final metal-coordinating water is more strongly bound than in the comparable nickel compound for which the complete removal of the water is very facile to achieve. Still, the metal sites in CPO-27-Mg are potentially accessible for various guest molecules.

Experimental Section

$[Mg(H_2dhtp)(H_2O)_2]$ (CPO-26-Mg): 2,5-Dihydroxyterephthalic acid (0.198 g, 1×10^{-3} mol) and ethanol (10 mL) were placed in the Teflon inlet of an autoclave. An aqueous sodium hydroxide solu-

tion (2 mL, 1 mol L^{-1}) was added to this suspension while stirring. A solution of magnesium nitrate hexahydrate (0.256 g, 1×10^{-3} mol) in water (3 mL) was added. The autoclave (filling level ca. 50%) was sealed and the mixture allowed to react at 110 °C for 3 d. Filtration yielded large transparent light yellow crystals. The purity of the product was checked by comparison of the observed powder X-ray diffractogram with the calculated pattern from the single-crystal structure determination.

$[Mg_2(dhtp)(H_2O)_2]\cdot 8H_2O$ (CPO-27-Mg): 2,5-Dihydroxyterephthalic acid (0.149 g, 0.75×10^{-3} mol) was dissolved in THF (10 mL) in the Teflon inlet of an autoclave. An aqueous sodium hydroxide solution (3 mL, 1 mol L^{-1}) was added to this solution while stirring. Magnesium nitrate hexahydrate (0.384 g, 1.5×10^{-3} mol) was dissolved in water (3 mL) and added to the Teflon inlet, upon which a yellow precipitate formed. The autoclave was sealed (filling level ca. 50%) and the mixture allowed to react at 110 °C for 3 d. Filtration yielded a light yellow substance of small, needle-shaped crystals (yield 0.200 g, 63% based on Mg). $C_4H_{11}MgO_8$ (211.43): calcd. C 22.72, H 5.24, Mg 11.50, O 60.54; found C 23.43, H 4.87, Mg 12.63, O 49.80. We ascribe the low value found for the O content to the formation of magnesium oxide from which the oxygen was not liberated for detection.

Crystal Structure Determination: Intensity data of a single crystal of CPO-26-Mg were collected with a Bruker D8 diffractometer with Apex II CCD area detector at room temperature by using Mo-K_α radiation. The data was processed with the SAINT software[44] and corrected for absorption with SADABS.[45] Structure solution and parameter refinement were performed by using the SHELXTL97 software suite.[46] The structures were solved by direct methods, and parameters were refined by using full-matrix least squares against $|F|^2$. All non-hydrogen atoms were refined by allowing for anisotropic displacement. Hydrogen atoms were located from difference maps. Their positional and isotropic thermal displacement parameters were freely refined. Crystallographic data are summarized in Table 3. Crystallites of CPO-27-Mg were too small for structure determination by single-crystal methods. Therefore, high-resolution powder X-ray diffraction data was recorded at the Swiss-Norwegian beamline (SNBL/BM01) at the European Synchrotron radiation Source (ESRF), Grenoble, France. The synchrotron source operated with an average energy of 6 GeV and a current beam of typically 200 mA. The SNBL received its radiation from a bending magnet in the storage ring. The incident X-ray wavelength was 0.49946 Å. Data collection was performed over the angular range of 2θ = 0.5–32.5° with a step width of 0.002° at room temperature. The powder diffraction pattern strongly resembled the patterns of the compounds $[M_2(dhtp)(H_2O)_2]\cdot 8H_2O$, CPO-27-M (M = Co, Ni). Indexation yielded a rhombohedral unit cell with lattice parameters very similar to the aforementioned compounds, whose structure was, therefore, chosen as starting model to determine the structure of CPO-27-Mg by Rietveld analysis. The GSAS program[47] was used to determine peak profiles and precise lattice parameters by LeBail fit of the pattern and subsequent full Rietveld refinement of the structure with the help of the EXPGUI graphical user interface.[48] Hydrogen atoms were not included in the model. They were rudimentally accounted for by setting the site occupation factor of the free solvent water molecules in the channel to 1.25. The final difference plot is shown in Figure 7, and crystallographic details are listed in Table 4. The seemingly large amplitude of the difference curve at the first reflection is due to the extreme asymmetric shape of the peak and the concomitant difficulty of describing its shape accurately. Molecular geometry calculations were performed with PLATON.[49] Topological analyses were per-

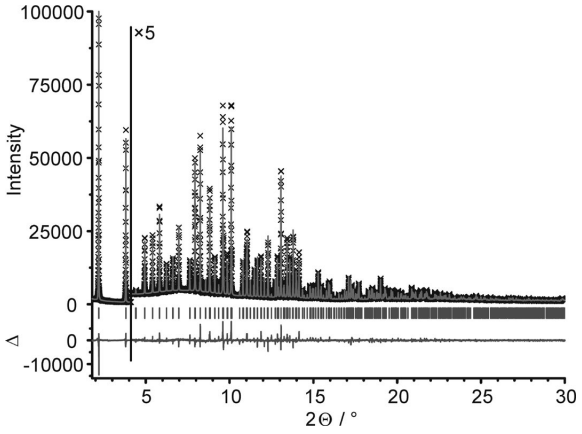

Figure 7. Scattered synchrotron radiation intensities for CPO-27-Mg as a function of the diffraction angle 2θ (crosses: observed pattern; grey line: best Rietveld-fit profile; line below pattern and tick marks: difference curve between observed and calculated profiles; tick marks: reflection positions). Intensities and difference plot of the high-angle part are enlarged by a factor of 5.

Table 3. Crystallographic data for the single-crystal structure solution of $[Mg(H_2dhtp)(H_2O)_2]$, CPO-26-Mg.

Empirical formula	$C_8H_8MgO_8$
Formula mass [g/mol]	256.45
Space group	*C*2/*c*
Z	4
a [Å]	8.349(3)
b [Å]	16.645(6)
c [Å]	6.997(2)
β [°]	108.236(3)
V [Å^3]	923.6(5)
$\rho_{calcd.}$ [g cm^{-3}]	1.844
μ [mm^{-1}]	0.23
λ [Å]	0.49946
2θ range [°]	4.9–55
No. of reflections	3823
No. of independent reflections	1051 (R_{int} = 0.035)
No. of observed reflections [$I > 2\sigma(I)$]	753
No. of parameters	94
R_1 [$I > 2\sigma(I)$ (all data)]	0.0355/0.0593
wR_2 [$I > 2\sigma(I)$ (all data)]	0.0815/0.0887
GOF	0.982
$\Delta\rho_{max}/\Delta\rho_{min}$ [e Å^{-1}]	0.30/–0.29

Table 4. Crystallographic data for the Rietveld refinement of $[Mg_2(dhtp)(H_2O)_2]\cdot 8H_2O$, CPO-27-Mg.

Empirical formula	$C_4H_{11}MgO_8$
Formula mass [g/mol]	211.43
Space group	$R\bar{3}$
Z	18
a [Å]	26.02607(6)
b [Å]	26.02607
c [Å]	6.758722(30)
β [°]	120
V [Å^3]	3964.719(17)
λ [Å]	0.71073
2θ range [°]	0.5–32.5
No. of reflections	1028
R_p	0.0543
R_{wp}	0.0720
$R(F^2)$	0.1011

formed with the program TOPOS.[50] CCDC-668973 and -668974 contain the supplementary crystallographic data for this paper. These data can be obtained free of charge from The Cambridge Crystallographic Data Centre via www.ccdc.cam.ac.uk/data_request/cif.

Variable-Temperature Powder X-ray Diffraction: Polycrystalline samples were filled in capillaries of 0.3 or 0.5 mm diameter and measured with a Siemens D5000 diffractometer. A steady air flow was passed through a furnace placed underneath the sample in such a way that the heating zone covered the X-ray beam width. The actual temperature at the sample was determined by measuring silver powder as external standard at different temperatures. To prepare the samples, the bottom ca. 1.5 cm of the capillary that were outside the X-ray beam and heating zone were filled with quarz glass to eliminate any possible influence of decomposition reactions occurring outside the heated and irradiated parts of the sample and to prevent excessive heat transfer in the silver sample during calibration. On top of the quarz glass, a sufficient amount of sample was placed to span the beam width. Some glass fibers were added to fix the sample in position. A specially modified sample holder which allows for a flow of gas to pass through the capillary containing the sample was used for the measurements under nitrogen gas.[51] In that case, glass fibers were placed on both sides of the sample within the capillary, and silver was used as internal standard for temperature calibration. The same setup was used for the measurements in dynamic vacuum for which the line leading to the goniometer head with the in-situ sample holder was connected to a rotary vane pump instead of the nitrogen gas supply. The heating rate of the experiments in the dynamic vacuum was 16 °C/h, whereas it was 10 °C/h in air. Two different heating rates of 6 and 16 °C/h were employed for experiments under nitrogen to yield essentially identical results. The variable-temperature diffraction data was analyzed and processed for presentation with the aid of the program Powder3D.[52]

Dehydration/Re-hydration Experiments: A custom-built apparatus equipped with a Cahn-200 balance was used to investigate the reversibility of dehydration of the porous compound CPO-27-Mg. It allowed for the easy removal of the furnace and switching between different types of gases, e.g. dry nitrogen gas and argon gas carrying water vapor, which is obtained by passing the argon gas through a flask filled with water. The heating rate was 1 °C/min. Prior to the experiment, the sample was exposed to the humid gas for ca. 90 min at room temperature until approximate weight constancy was reached. In this state, the channels were assumed to be fully loaded with water corresponding to the formula $[Mg_2(dhtp)(H_2O)]\cdot 8H_2O$. The gas was then switched to dry nitrogen and heating commenced. The sample was kept at the final temperature for various amounts of time to observe the long-term stability under these conditions. Then, the furnace was removed, and the gas was switched to humid argon again. Once the water uptake had ceased, the whole procedure was repeated again on the same sample by varying tempering temperature and time.

Nitrogen Adsorption: Several samples of CPO-27-Mg in the range of 10–160 mg were measured with a BELSORP-miniII at 77 K. The samples were subjected to miscellaneous activation procedures in a dynamic vacuum prior to the adsorption experiment. Pre-treatment temperatures ranged from 110 to 300 °C, and they were applied for 700–1000 min. The samples showing the highest surface areas had been immersed for 3–15 d in water or methanol until shortly before the experiment. Details of the pre-treatment conditions and results of the gas adsorption experiments are given in the Supporting Information.

Supporting Information (see footnote on the first page of this article): Structure drawing of CPO-26-Mg depicting displacement parameters, comparison of observed and calculated powder X-ray diffraction patterns of CPO-26-Mg, details of pre-treatment conditions and results of gas adsorption experiments performed on CPO-27-Mg.

Acknowledgment

Assistance from Wouter van Beek and Hermann Emmerich at the Swiss-Norwegian Beamlines, ESRF, and the financial support by the Research Council of Norway through the NANOMAT program (grants 153869/S10 & 182056/S10) and the EU through the NMP program (MOFCAT project, contract no. NMP4-CT-2006-033335) are gratefully acknowledged.

[1] S. L. James, *Chem. Soc. Rev.* **2003**, *32*, 276–288.
[2] S. Kitagawa, R. Kitaura, S. Noro, *Angew. Chem. Int. Ed.* **2004**, *43*, 2334–2375.
[3] J. L. C. Rowsell, O. M. Yaghi, *Angew. Chem. Int. Ed.* **2005**, *44*, 4670–4679.
[4] U. Mueller, M. Schubert, F. Teich, H. Puetter, K. Schierle-Arndt, J. Pastré, *J. Mater. Chem.* **2006**, *16*, 626–636.
[5] K. M. Thomas, *Catal. Today* **2007**, *120*, 389–398.
[6] K. Seki, S. Takamizawa, W. Mori, *Chem. Lett.* **2001**, *30*, 332–333.
[7] M. Eddaoudi, J. Kim, N. Rosi, D. Vodak, J. Wachter, M. O'Keeffe, O. M. Yaghi, *Science* **2002**, *295*, 469–472.
[8] H. K. Chae, D. Y. Siberio-Pérez, J. Kim, Y. Go, M. Eddaoudi, A. J. Matzger, M. O'Keeffe, O. M. Yaghi, *Nature* **2004**, *427*, 523–527.
[9] D. N. Dybtsev, H. Chun, K. Kim, *Angew. Chem. Int. Ed.* **2004**, *43*, 5033–5036.
[10] G. Férey, C. Mellot-Draznieks, C. Serre, F. Millange, J. Dutour, S. Surblé, I. Margiolaki, *Science* **2005**, *309*, 2040–2042.
[11] X. Lin, J. Jia, X. Zhao, K. M. Thomas, A. J. Blake, G. S. Walker, N. R. Champness, P. Hubberstey, M. Schröder, *Angew. Chem. Int. Ed.* **2006**, *45*, 7358–7364.
[12] M. Latroche, S. Surblé, C. Serre, C. Mellot-Draznieks, P. L. Llewellyn, J.-H. Lee, J.-S. Chang, S. H. Jhung, G. Férey, *Angew. Chem. Int. Ed.* **2006**, *45*, 8227–8231.
[13] C. Serre, C. Mellot-Draznieks, S. Surblé, N. Audebrand, Y. Filinchuk, G. Férey, *Science* **2007**, *315*, 1828–1831.
[14] H. Chun, D. N. Dybtsev, H. Kim, K. Kim, *Chem. Eur. J.* **2005**, *11*, 3521–3529.
[15] J. Baier, U. Thewalt, *Z. Anorg. Allg. Chem.* **2002**, *628*, 315–321.
[16] J. Baier, U. Thewalt, *Z. Anorg. Allg. Chem.* **2002**, *628*, 1890–1894.
[17] B. H. Hamilton, K. A. Kelly, W. Malasi, C. J. Ziegler, *Inorg. Chem.* **2003**, *42*, 3067–3073.
[18] I. Imaz, G. Bravic, J.-P. Sutter, *Dalton Trans.* **2005**, 2681–2687.
[19] A. Grirrane, A. Pastor, E. Álvarez, A. Galindo, *Inorg. Chem. Commun.* **2005**, *8*, 453–456.
[20] S. Gao, J.-W. Liu, L.-H. Huo, H. Zhao, *Acta Crystallogr., Sect. E* **2005**, *61*, m1117–m1119.
[21] M. Dincă, J. R. Long, *J. Am. Chem. Soc.* **2005**, *127*, 9376–9377.
[22] M. Viertelhaus, C. E. Anson, A. K. Powell, *Z. Anorg. Allg. Chem.* **2005**, *631*, 2365–2370.
[23] M. Viertelhaus, P. Adler, R. Clérac, C. E. Anson, A. K. Powell, *Eur. J. Inorg. Chem.* **2005**, 692–703.
[24] I. Senkovska, S. Kaskel, *Eur. J. Inorg. Chem.* **2006**, 4564–4569.
[25] J. A. Rood, B. C. Noll, K. W. Henderson, *Inorg. Chem.* **2006**, *45*, 5521–5528.
[26] S. Maa, J. A. Fillingera, M. W. Ambrogioa, J.-L. Zuob, H.-C. Zhou, *Inorg. Chem. Commun.* **2007**, *10*, 220–222.
[27] J. A. Rood, B. C. Noll, K. W. Henderson, *Main Group Chem.* **2007**, *5*, 21–30.

[28] J. A. Rood, W. C. Boggess, B. C. Noll, K. W. Henderson, *J. Am. Chem. Soc.* **2007**, *129*, 13675–13682.
[29] Z. Hulvey, A. K. Cheetham, *Solid State Sci.* **2007**, *9*, 137–143.
[30] L. Hai-Ye, L. Bei-Ling, J. Yi-Min, Z. Shu-Hua, L. Jun-Xia, *Chin. J. Struct. Chem.* **2007**, *26*, 907–910.
[31] A. Mesbah, C. Juers, F. Lacouture, S. Mathieu, E. Rocca, M. François, J. Steinmetz, *Solid State Sci.* **2007**, *9*, 322–328.
[32] K. C. Kam, K. L. M. Young, A. K. Cheetham, *Cryst. Growth Des.* **2007**, *7*, 1522–1532.
[33] R. P. Davies, R. J. Less, P. D. Lickiss, A. J. P. White, *Dalton Trans.* **2007**, 2528–2535.
[34] D.-J. Zhang, T. Y. Song, P. Zhang, J. Shi, Y. Wang, L. Wang, K. R. Ma, W. R. Yin, J. Zhao, Y. Fan, J. N. Xu, *Inorg. Chem. Commun.* **2007**, *10*, 876–879.
[35] I. Senkovska, J. Fritsch, S. Kaskel, *Eur. J. Inorg. Chem.* **2007**, 5475–5479.
[36] J. Zhang, S. Chen, H. Valle, M. Wong, C. Austria, M. Cruz, X. Bu, *J. Am. Chem. Soc.* **2007**, *129*, 14168–14169.
[37] C. A. Williams, A. J. Blake, C. Wilson, P. Hubberstey, M. Schröder, *Cryst. Growth Des.* **2008**, *8*, 911–922.
[38] N. L. Rosi, J. Kim, M. Eddaoudi, B. Chen, M. O'Keeffe, O. M. Yaghi, *J. Am. Chem. Soc.* **2005**, *127*, 1504–1518.
[39] P. D. C. Dietzel, Y. Morita, R. Blom, H. Fjellvåg, *Angew. Chem. Int. Ed.* **2005**, *44*, 6354–6358.
[40] P. D. C. Dietzel, R. E. Johnsen, R. Blom, H. Fjellvåg, *Chem. Eur. J.* **2008**, *14*, 2389–2397.
[41] P. D. C. Dietzel, B. Panella, M. Hirscher, R. Blom, H. Fjellvåg, *Chem. Commun.* **2006**, 959–961.
[42] P. D. C. Dietzel, R. Blom, H. Fjellvåg, *Dalton Trans.* **2006**, 2055–2057.
[43] N. E. Ghermani, G. Morgant, J. d'Angelo, D. Desmaele, B. Fraisse, F. Bonhomme, E. Dichi, M. Sgahier, *Polyhedron* **2007**, *26*, 2880–2884.
[44] *SAINT:* Area-Detector Integration Software, Bruker AXS, Madison, WI, **2004**.
[45] *SADABS:* Area-Detector Absorption Correction, Bruker AXS, Madison, WI, **2004**.
[46] G. M. Sheldrick, *SHELXTL – Program suite for the solution and refinement of crystal structures*, Bruker AXS, Madison, WI, **2004**.
[47] A. C. Larson, R. B. V. Dreele, *General Structure Analysis System (GSAS)*, Los Alamos National Laboratory Report LAUR 86-748, **2000**.
[48] B. H. Toby, *J. Appl. Crystallogr.* **2001**, *34*, 210–213.
[49] A. L. Spek, *J. Appl. Crystallogr.* **2003**, *36*, 7–13.
[50] V. A. Blatov, *Cryst. Rev.* **2004**, *10*, 249–318.
[51] P. Norby, *J. Am. Chem. Soc.* **1997**, *119*, 5215–5221.
[52] B. Hinrichsen, R. E. Dinnebier, M. Jansen, *Z. Krist. Suppl. 23 (EPDIC IX proceeding)* **2006**, 231–236.

Received: November 29, 2007
Published Online: July 4, 2008

